

# Non-equilibrium Transport in dissipative one-dimensional Nanostructures

Hui Dai<sup>1</sup> and Dirk K. Morr<sup>1,2</sup>

<sup>1</sup> *Department of Physics and James Franck Institute, University of Chicago, Chicago, IL 60637, USA*

<sup>2</sup> *University of Illinois at Chicago, Chicago, IL 60607, USA*

(Dated: June 11, 2010)

We study the non-equilibrium transport properties of a one-dimensional array of dissipative quantum dots. Using the Keldysh formalism, we show that the dots' dissipative nature leads to a spatial variation of the chemical potential, which in disordered arrays, breaks the invariance of the current,  $I$ , under bias reversal. Moreover, the array's nanoscopic size results in an algebraic low-temperature dependence of  $I$ . Finally, we show that a local Coulomb interaction splits the dots' electronic levels, resulting in a Coulomb blockade, which is softened with increasing dissipation and array size.

PACS numbers: 73.63.-b, 73.63.Kv, 73.22.-f, 73.23.-b

Arrays of metallic [1, 2] or semiconducting [3, 4] quantum dots (QDs) have attracted significant interest due to the unprecedented experimental control in assembling such arrays, and the resulting ability to custom-design their electronic structure and transport properties [5, 6]. The continued miniaturization of such arrays, important for many applications in quantum computation [7] and nanoelectronics [5], raises the important question of how the non-equilibrium transport properties in nanoscopic arrays differ from those in mesoscopic ones and how they evolve across different length scales. Nanoscale arrays also provide a unique opportunity to study how the local interplay between dissipation [8, 9], disorder, and Coulomb interaction affects their global transport properties. Investigating the evolution of these properties across different length scales might also hold the key to identifying the (yet unresolved) origin of the low-temperature conductivity observed in mesoscopic QD arrays [1, 3] which is ascribed either to some variable-range hopping (VRH) [2, 3] or cotunneling [1, 10] mechanism.

In this Letter, we address the above questions by studying the non-equilibrium transport properties of one-dimensional (1D), nanoscale arrays of dissipative QDs, as schematically shown in Fig. 1(a). Using the Keldysh

Green's function formalism [11, 12], we demonstrate that the interplay between dissipation, Coulomb interaction, and disorder gives rise to a series of novel non-equilibrium quantum effects. In particular, the dots' dissipative nature leads to a spatial variation of the chemical potential,  $\mu$ , reflecting the array's resistance, which changes qualitatively with increasing disorder, and breaks the invariance of the current under bias reversal. Moreover, the array's nanoscopic size yields an algebraic low-temperature dependence of the current in disordered arrays, in contrast to the exponential scaling observed in mesoscopic arrays [1, 3]. Finally, we demonstrate that a local Coulomb interaction results in a splitting of a dot's energy level, which continuously varies with the level's occupation. This splitting gives rise to a Coulomb blockade in the charge transport, which is softened with increasing dissipation and/or size of the array. These results provide important new insight into the complex non-equilibrium transport properties of nanoscale systems.

We consider a one-dimensional array of  $N$  quantum dots connected to a left and right lead [Fig. 1(a)] whose Hamiltonian is given by  $\mathcal{H} = \mathcal{H}_c + \mathcal{H}_{ph} + \mathcal{H}_{leads}$  where

$$\begin{aligned} \mathcal{H}_c = & \sum_{j,\sigma} \varepsilon(j) c_{j,\sigma}^\dagger c_{j,\sigma} + U \sum_j \hat{n}_{j,\uparrow} \hat{n}_{j,\downarrow} \\ & - \sum_{j,\sigma} t c_{j,\sigma}^\dagger c_{j+1,\sigma} - \sum_{\sigma,\nu=R,L} t_\nu c_{n_\nu,\sigma}^\dagger d_{\nu,\sigma} + H.c. \end{aligned} \quad (1)$$

Here  $c_{j,\sigma}^\dagger$  and  $d_{\nu,\sigma}^\dagger$  create an electron with spin  $\sigma$  on dot  $j$  and lead  $\nu$  ( $\nu = R, L$ ), respectively. We assume for simplicity that on each dot, there is only a single electronic state with energy  $\varepsilon(j)$  that is relevant for charge transport, as is the case in semiconducting QDs [9].  $U$  represents the strength of the local (intra-dot) Coulomb interaction, and  $t$  is the hopping matrix element between neighboring dots.  $t_\nu$  describes the coupling of the array to the leads with  $n_{L(R)} = 1(N)$ . Finally,  $\mathcal{H}_{ph}$  and  $\mathcal{H}_{leads}$  represent the local electron-phonon interaction on each dot and the leads' electronic structure, respectively.

In order to study the array's non-equilibrium transport properties, we consider a (symmetric) bias,  $V = \mu_L - \mu_R$ ,

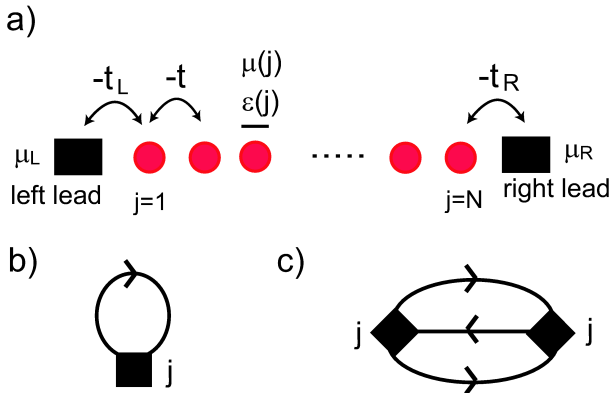


FIG. 1: (a) One-dimensional array of quantum dots coupled to two leads. (b) First and (c) second order fermionic self-energy corrections due to a local Coulomb interaction.

across the array arising from different chemical potentials in the left and right leads with  $\mu_R = -\mu_L$ . The resulting current between dots  $j$  and  $(j+1)$  is given by [13]

$$I_{j,j+1} = -\frac{e}{\hbar} t \int_{-\infty}^{+\infty} \frac{d\omega}{2\pi} \text{Re} \left[ \hat{F}_{j,j+1}(\omega) \right]. \quad (2)$$

Here,  $\hat{F}$  is the full Keldysh Green's functions matrix of the entire array, which accounts for (electron-phonon and Coulomb) interactions, electronic hopping between dots and the coupling to the leads. Since scanning tunneling spectroscopy (STS) on QD arrays [9] reported that intra-dot interactions are larger than the inter-dot electronic hopping [9], we include the former first in the perturbative calculation of  $\hat{F}$ , in contrast to the limit considered previously [14, 15]. Moreover, STS experiments [8, 9] also reported significant energy broadening (i.e., dissipation) of the dots' electronic states (likely arising from electron-phonon coupling) which is only weakly temperature and energy dependent, and remains substantial even for  $T \rightarrow 0$  [9]. We account for the dissipation by introducing a (phenomenological) lifetime,  $\Gamma^{-1}$ , of the dots' electronic states (we take  $\varepsilon$  to include a possible shift due to the electron-phonon interaction) [14, 15]. The Green's function of a single (isolated) dot is then (the effects of a Coulomb interaction are discussed below)

$$g_r^{-1}(\omega) = \omega - (\varepsilon - \mu) + i\Gamma. \quad (3)$$

Including next the electronic hopping between the dots and the coupling to the leads, we obtain

$$\hat{F} = (1 - \hat{g}_r \hat{t})^{-1} \hat{f} (1 - \hat{t} \hat{g}_a)^{-1}. \quad (4)$$

Here,  $\hat{g}_{r,a}$  and  $\hat{f}$  are the (diagonal) retarded, advanced and Keldysh Greens function matrices describing the decoupled ( $t = t_\nu = 0$ ) dots and leads, respectively, with

$$\hat{f}(\omega) = 2i [1 - 2\hat{n}_F(\omega)] \text{Im} [\hat{g}_r(\omega)]. \quad (5)$$

$\hat{n}_F$  is a diagonal matrix containing the dots' and leads' Fermi-distribution functions, and  $\hat{t}$  is the symmetric hopping matrix. While the results shown below were obtained in arrays with  $N = 20$  dots, we found qualitatively similar behavior up to the largest arrays ( $N = 150$ ) we studied. For concreteness, we take  $t = t_{R,L} = 0.3E_0$  and  $\Gamma = 0.05E_0$ , unless otherwise specified.

In order to understand an array's transport properties, it is instructive to first consider its (equilibrium) electronic structure. To this end, we present in Fig. 2(a) the local density of states (LDOS),  $N_j(\omega) = -\text{Im}\hat{G}_{jj}^r(\omega)/\pi$  where  $\hat{G}_r = (1 - \hat{g}_r \hat{t})^{-1} \hat{g}_r$  of a non-disordered array with  $N = 20$  dots. The array's nanoscopic 1D structure gives rise to a significant curvature of the band (see discussion below), with the LDOS exhibiting the precursors of the

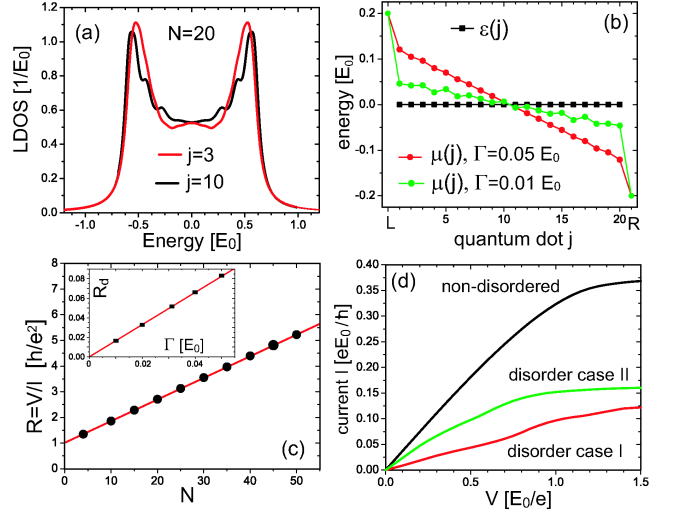


FIG. 2: QD array with  $N = 20$ . (a)  $N_j(\omega)$  in equilibrium with  $\varepsilon(j) = \mu(j) = 0$ . (b)  $\mu(j)$ ,  $\varepsilon(j)$  for  $V = 0.4E_0/e$  and different  $\Gamma$ .  $L$  and  $R$  refer to the left and right leads, respectively. (c) Resistance  $R = V/I$  as a function of  $N$ . Inset:  $R_d$  as a function of  $\Gamma$ . (d)  $IV$ -curve for a non-disordered array and two different disorder realizations with  $s = 0.2E_0$ .

$1/\sqrt{E}$ -divergence characteristic of an array with  $N = \infty$ .

We next discuss the array's non-equilibrium transport properties. For a given bias  $V$ , charge conservation in the steady-state requires that all currents  $I_{j,j+1}$  be the same. For dissipative QDs with  $\Gamma \neq 0$ , this requirement can only be satisfied by allowing spatial variations in the local chemical potential [16],  $\mu(j)$ , of each dot [Fig. 2(b)], which enters in the calculation of  $I_{j,j+1}$  through  $\hat{f}(\omega)$  in Eqs.(4) and (5). Hence,  $\mu$  should be interpreted as the electro-chemical potential and its difference between two adjacent dots as the change in the electrostatic potential due to the array's resistance. As expected, the spatial variation of  $\mu$  decreases with decreasing  $\Gamma$  and vanishes for a non-dissipative array with  $\Gamma \rightarrow 0$  [12]. A plot of the resistance,  $R = V/I$ , as a function of  $N$  [Fig. 2(c)] reveals a linear relationship  $R = 2R_I + R_d N$ , with  $R_I \approx 0.50\hbar/e^2$  and  $R_d \approx 0.084\hbar/e^2$  being the interface resistance and resistance per dot, respectively, demonstrating that the array behaves as a series of resistors. Since  $R_I \gg R_d$ , the change in  $\mu$  at the interface is significantly larger than that between dots, in agreement with Fig. 2(b). Moreover,  $R_d \sim \Gamma$  (see inset) demonstrates that it is the dissipative nature of the QDs that is responsible for the array's resistance. Finally, a plot of the  $IV$ -curve in Fig. 2(d) shows ohmic behavior,  $I \sim V$ , at low bias while  $I$  becomes basically independent of  $V$  once  $V$  exceeds the electronic band width,  $W \approx 4t = 1.2E_0$ , of the array.

Disorder in an array can emerge from non-uniformity in the dots' spacing or size, leading to variations in  $t$  and  $\varepsilon(j)$ , respectively. Below, we consider the latter case, which has a more profound effect on the array's trans-

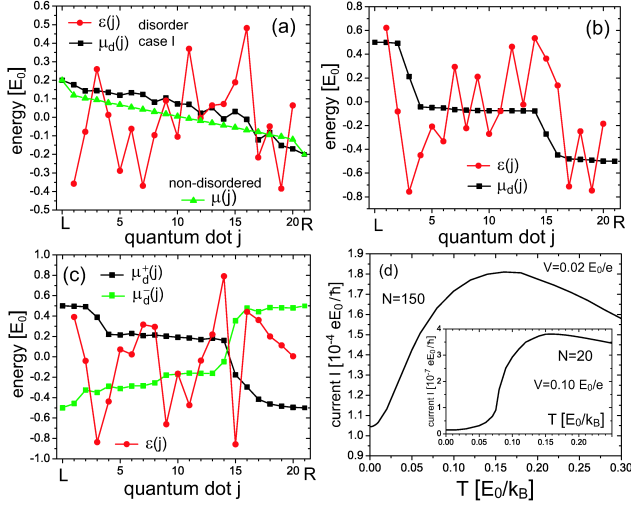


FIG. 3:  $\varepsilon(j)$ ,  $\mu_d(j)$  for (a) a non-disordered array and disorder case I, and (b) for a strongly disordered array with  $t = \Gamma = 0.01E_0$ , and  $s = 0.5E_0$ . (c)  $\varepsilon(j)$ ,  $\mu_d^\pm(j)$  for a disordered array under bias reversal. (d)  $I(T)$  for an array with  $N = 150$  at intermediate disorder with  $s = t = 0.3E_0$  and  $\Gamma = 0.05E_0$ . Inset:  $I(T)$  for the strongly disordered array of (b).

port properties, and take  $\varepsilon(j)$  to be Gaussian (disorder-) distributed with average value  $\langle \varepsilon(j) \rangle = 0$  and standard deviation  $s$ . The  $IV$ -curve for two realizations of intermediate disorder ( $t \sim s$ ), case I and II with  $s = 0.2E_0$ , are plotted in Fig. 2(d) [ $\varepsilon(j)$  for case I is shown in Fig. 3(a)]. While in both cases, the current is suppressed by disorder, the extent of the suppression depends on the specific disorder realization. The microscopic origin of this suppression lies in the diminished hybridization of electronic states between neighboring dots due to the differences in their energies,  $\varepsilon(j)$ . In Fig. 3(a) we present  $\varepsilon(j)$  and  $\mu_d(j)$  for disorder case I together with  $\mu(j)$  for the non-disordered array. Surprisingly,  $\mu_d(j)$  does not differ significantly from  $\mu(j)$ , and in particular, does not track the variations in  $\varepsilon(j)$ . The reason for this robustness of  $\mu_d$  is that in the intermediate disorder case, electrons can tunnel even through those dots where  $|\varepsilon|$  is large. In contrast, in the strong disorder limit,  $t, \Gamma \ll s$ , shown in Fig. 3(d),  $\mu_d(j)$  exhibits step-like changes between those neighboring dots where the variation in  $\varepsilon(j)$  is the largest. This is expected since large spatial variations of  $\varepsilon(j)$  indicate the regions of largest resistance in the array, with concomitant large (potential) changes in  $\mu_d(j)$ .

The interplay between disorder and dissipation gives rise to an interesting novel quantum phenomenon in which the invariance of the current's magnitude is broken under bias reversal. To demonstrate this effect, we present in Fig. 3(c) the chemical potentials,  $\mu_d^\pm(j)$ , in a dissipative, disordered array for two different bias  $V_\pm = \pm E_0/e$ . Due to the combination of disorder and dissipation,  $\mu_d^+$  and  $\mu_d^-$  are not related by a spatial sym-

metry, implying that the corresponding currents are in general different: in Fig. 3(c), the current for positive bias  $V_+$  is  $I_+ = 0.0089eE_0/\hbar$ , while for  $V_-$  one finds  $I_- = -0.0261eE_0/\hbar$ . We note that the invariance is restored either in a non-disordered dissipative array, or in a non-dissipative ( $\Gamma = 0^+$ ) disordered array. In the latter case, the current is independent of  $\mu$  [12] and  $\mu_d^\pm(j) \equiv 0$  again satisfies the spatial symmetry.

The temperature dependence of  $I$  is generally determined by both disorder and interaction effects, with the latter being represented by  $\Gamma$ . However, when disorder becomes stronger than dissipation (i.e.,  $s \gtrsim \Gamma$ ), we find that the current is predominantly determined by the former, and becomes essentially independent of  $\Gamma$ . Thus, in calculating  $I(T)$ , we can neglect the temperature dependence of interaction effects, i.e.,  $\Gamma(T)$ , as was previously assumed in Refs.[17, 18]. In the limit of intermediate disorder,  $\Gamma \ll t \sim s$ , and for  $k_B T \ll s$ ,  $I(T)$  possesses an algebraic temperature dependence,  $I(T) = I_0 + BT^2$ , as shown in Fig. 3(d) for an array with  $N = 150$  dots. This algebraic dependence is the lowest order (in  $T$ ) contribution arising from the frequency dependence of the Green's functions entering Eq.(4), which in turn arises from the finite 1D structure of the array [this frequency dependence is also present in the LDOS of Fig. 2(a)]. In the strong disorder limit,  $\Gamma, t \ll s$  (see inset of Fig. 3(d)), the algebraic temperature dependence of  $I(T)$  at small  $T$  is followed by a more rapid increase at larger temperatures, which can be described by an activated behavior over some limited temperature range. We note that the absence of an exponential VRH temperature scaling [17, 18], is one of the characteristic hallmarks of nanoscale systems. Not only would the algebraic contribution to  $I(T)$  dominate any exponential scaling for  $T \rightarrow 0$ , but VRH scaling also assumes that a disordered system is characterized by a single parameter, the localization length, and thus neglects spatial fluctuations in the disorder. These fluctuations are, however, highly relevant in nanoscale systems due to the lack of disorder self-averaging, resulting in different  $IV$ -curves for different disorder realizations with the same  $s$  [Fig. 2(d)]. Work is currently under way to identify the characteristic size of the QD array at which disorder self-averaging will lead to a crossover from algebraic to VRH scaling of  $I(T)$ .

We next study the effects of a local Coulomb interaction by including the first [Fig. 1(b)] and second order [Fig. 1(c)] fermionic self-energy corrections in the local Green's functions entering Eq.(4). Based on the experimental STS results of Ref. [9], we take the Coulomb interaction to be weaker than the electron-phonon interaction, and thus take the internal fermionic lines of the diagrams in Figs. 1(b) and (c) to be given by the dissipative Green's function of Eq.(3). The first order diagram of Fig. 1(b) leads to an energy shift  $\bar{\varepsilon}_\sigma(j) = \varepsilon(j) + U n_{j,\bar{\sigma}}$  with  $n_{j,\sigma}$  being the electron occupation and  $\sigma, \bar{\sigma}$  being opposite spin quantum numbers. In contrast, the second order di-

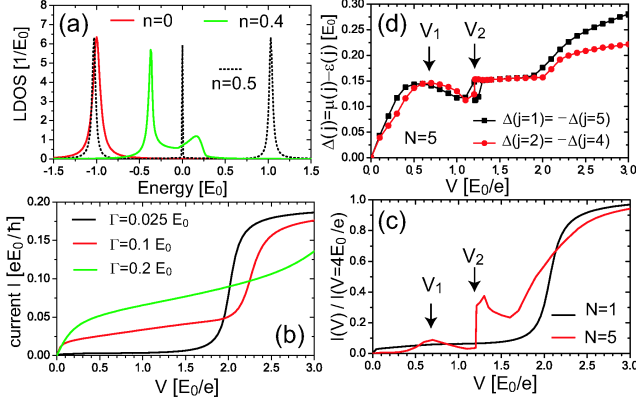


FIG. 4: (a) LDOS of a single dot with  $\Gamma = 0.05E_0$  for  $n_{j,\sigma} = 0, 0.4, 0.5$ . (b)  $IV$ -curve for an array with  $N = 1$  and different  $\Gamma$ . (c) Normalized  $IV$ -curve for arrays with  $N = 1$  and  $N = 5$  dots. (d)  $\Delta(j) = \mu(j) - \varepsilon(j)$  as a function of  $V$  for  $N = 5$ .

agram, for which an analytical form can be derived, leads to an energy splitting which depends on  $n_{j,\sigma}$ : for a completely empty or filled state, the splitting vanishes, while it is the largest for a half-filled state. To demonstrate the evolution of the dot's electronic structure with  $n_{j,\sigma}$ , we present in Fig. 4(a) the LDOS of a single dot [including the self-energy corrections of Figs. 1(b),(c)] for  $n_{j,\sigma} = 0.0, 0.4, 0.5$ , and  $U = 2E_0$  (the LDOS for occupation  $1 - n_{j,\sigma}$  is obtained via  $\omega \leftrightarrow -\omega$ ). For  $n_{j,\sigma} = 0$  ( $n_{j,\sigma} = 1$ ), the dot possess a single, doubly degenerate energy level at  $\omega = -E_0$  ( $\omega = +E_0$ ). As  $n_{j,\sigma}$  increases, this level shifts to larger energies, and a splitting emerges. For  $n_{j,\sigma} = 0.5$ , the state's spectral weight is predominantly located at  $\omega = \pm E_0$ , i.e., separated by  $U = 2E_0$ , while a small contribution of spectral weight is found at  $\omega = 0$ , which is a direct consequence of  $\Gamma \neq 0$ , and hence vanishes for  $\Gamma \rightarrow 0$ . This evolution of the LDOS with  $n_{j,\sigma}$  is identical to that of Ref. [19] for  $\Gamma = 0^+$ , but qualitatively differs from it for  $\Gamma \neq 0$ . The state's splitting, which is analogous to the Coulomb interaction driven suppression of the LDOS near the Fermi energy discussed by Efros and Shklovskii [18], is the origin of the Coulomb blockade observed in  $IV$  curves. For a single QD with  $\mu = 0$  and  $n_{j,\sigma} = 0.5$  [Fig. 4(b)], the dot's energy level is maximally split, and  $I$  is strongly suppressed until  $V$  exceeds  $U$ , thus manifesting the Coulomb blockade. The state's spectral weight at  $\omega = 0$  (due to  $\Gamma \neq 0$ ) leads to a non-zero  $I$  even for a  $V < U$ . The Coulomb blockade is softened both with increasing  $\Gamma$  [Fig. 4(b)] as well as with increasing number of dots  $N$  in the array, as shown in Fig. 4(c) for  $N = 5$ . In addition, in the latter case, new features appear for  $V < U$  which arise from changes in  $\Delta(j) = \mu(j) - \varepsilon(j)$ , where  $\Delta(j) = 0$  corresponds to  $n_{j,\sigma} = 0.5$  and thus a maximum splitting of the energy level. As  $\Delta(j)$  increases, this splitting is reduced, and  $I$  increases (and vice versa) as follows from a comparison

of Figs. 4(c) and (d). Therefore, the local maximum of  $I$  at  $V_1 \approx 0.7E_0/e$  coincides with that of  $\Delta(j)$ , while its sharp increase at  $V_2 \approx 1.2E_0$  reflects that of  $\Delta(j)$ . For  $V > V_2$ ,  $I$  decreases slightly due to an increasing separation between the dots' energy levels, but then increases again as  $V$  approaches the Coulomb gap,  $U$ .

In summary, we studied the non-equilibrium transport properties of a 1D array of dissipative QDs. We showed that the QDs' dissipative nature leads to a spatial variation of  $\mu(j)$ , reflecting the resistance of the array. In disordered arrays, this variation breaks the invariance of the current under bias reversal while the array's nanoscopic size results in an algebraic low-temperature dependence of  $I(T)$ . Finally, we showed that a local Coulomb interaction gives rise to a splitting of the dots' energy levels, and the emergence of a Coulomb blockade, which is softened with increasing dissipation and size of the array.

We would like to thank J. Figgins, I. Gruzberg, P. Guyot-Sionnest, H. Jaeger, L. Kadanoff, A. Kamenev, and G.P. Parravicini for stimulating discussions. D.K.M. would like to thank the Aspen Center for Physics for its hospitality during the final stage of this project. This work is supported by the U.S. Department of Energy under Award No. DE-FG02-05ER46225 (D.K.M) and by NSF MRSEC under Award No. 0820054 (H.D.).

- 
- [1] T. B. Tran *et al.*, Phys. Rev. Lett. **95**, 076806 (2005); T. B. Tran *et al.*, Phys. Rev. B **78**, 075437 (2008).
  - [2] A. Zabet-Khosousi *et al.*, Phys. Rev. Lett. **96**, 156403 (2006).
  - [3] D. Yu *et al.*, Phys. Rev. Lett. **92**, 216802 (2004); D. Yu *et al.*, Science **300**, 1277 (2003).
  - [4] A. J. Houtepen, D. Kockmann, and D. Vanmaekelbergh, Nano Letters **8**, 3516 (2008).
  - [5] A.N. Shipway *et al.*, Chemphyschem **1**, 18 (2000). (2008).
  - [6] I.S. Beloborodov *et al.*, Rev. Mod. Phys. **79**, 469 (2007).
  - [7] D. Loss and D.P. DiVincenzo, Phys. Rev. A **57**, 120 (1998).
  - [8] T. Maltezopoulos *et al.*, Phys. Rev. Lett. **91**, 196804 (2003).
  - [9] L. Jdira *et al.*, Phys. Rev. B **77**, 205308 (2008).
  - [10] I.S. Beloborodov *et al.*, arXiv:cond-mat/0501094, unpublished.
  - [11] J. Schwinger, J. Math. Phys. (N.Y.) **2**, 407 (1961); L.P. Kadanoff and G. Baym, Quantum Statistical Mechanics (Benjamin, New York, 1962); J. Rammer and H. Smith, Rev. Mod. Phys. **58**, 323 (1986).
  - [12] L.V. Keldysh, 1964, Zh. Eksp. Teor. Fiz. **47**, 1515 (1964) [Sov. Phys.—JETP **20**, 1018 (1965)];
  - [13] C. Caroli *et al.*, J. Phys. C: Solid St. Phys **4**, 916 (1971).
  - [14] A. Mitra *et al.*, Phys. Rev. B **69**, 245302 (2004).
  - [15] Z. Bihary and M. A. Ratner Phys. Rev. B **72**, 115439 (2005).
  - [16] M. Büttiker, Phys. Rev. B **32**, R1846 (1985).
  - [17] N. F. Mott, J. Non-Cryst. Solids **1**, 1 (1968).
  - [18] A. L. Efros and B. I. Shklovskii, J. Phys. C: Solid State Phys. **8**, L49 (1975).
  - [19] Y. Meir *et al.*, Phys. Rev. Lett. **66**, 3048 (1991).